Electronic Supplementary Material (ESI) for Sustainable Energy & Fuels.

Techno-economic and environmental assessment of BECCS in fuel generation for FT-fuel, bioSNG, and OMEx

Oluchi Emenike[a], Stavros Michailos[a], Kevin J Hughes[a], Derek Ingham[a], Mohamed Pourkashanian[a]

[a]Energy 2050, Department of Mechanical Engineering, Faculty of Engineering, University of Sheffield, Sheffield S3 7RD, UK

Supplementary Information

S1 Biomass preparation

Figure A is the process flow diagram (PFD) for the biomass preparation section. The biomass preparation section covers the chopping, grinding, and drying of biomass. The moisture in biomass is reduced to 10% using steam. The amount of steam required, and the final moisture content are set by a calculator block. The moisture removed and the steam used in drying are separated from the biomass feed in an adiabatic flash unit.

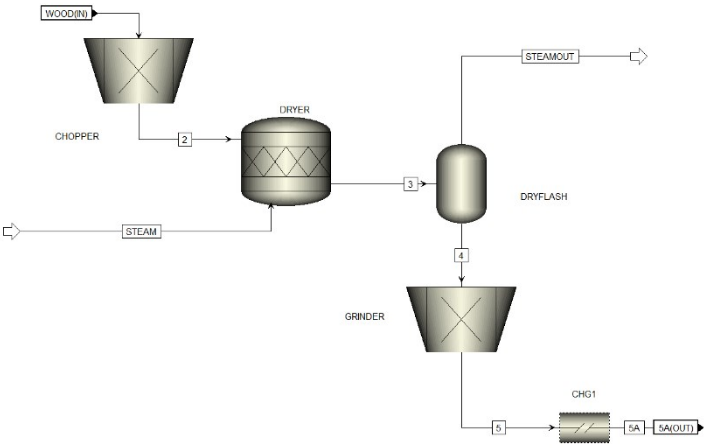

Figure A: Aspen Plus flowsheet for biomass preparation.

S.2 Gasification modelling

S.2.1 Dual fluidised gasifier model

An indirect gasifier in the form of a dual fluidised bed gasifier is modelled and validated here. The dual fluidised bed (DFB) gasifier has been used in several projects pertaining to biofuel production from biomass gasification (Goteborg, Gussing, Varnamo, MILENA etc) [1,2]. The DFB gasifier in this study is based on the Göteborg biomass gasification project (GoBiGas) plant in Sweden that produced bioSNG from woody biomass gasification [3]. The DFB gasifier is a gasifier where gasification occurs in one fluidised bed and the heat for gasification is generated in the other fluidised bed. In this gasifier, since air is introduced in a different zone, the syngas is practically nitrogen free. While thermodynamic modelling is suitable for first estimates and determining the limits of the system, it underestimates the hydrocarbons (C_1, C_2, tars) production and overestimates hydrogen production from gasification [4–6]. Kinetic modelling, which is more suitable for gasifier design, helps to reduce the inaccuracies but this is more complex and cannot be easily applied [7–9]. In this model, to reduce the inaccuracies from thermodynamic modelling, non-ideal corrections are applied to account for the formation of hydrocarbons especially methane and tar. This is based on similar equilibrium modelling techniques in [10–12]. An RStoic block is introduced in the model where the fractional carbon conversions of each reaction is set to match the experimental data in Alamia et al. [13] and simulate hydrocarbons formation to account for the non-equilibrium nature of gasification. This step is important in accounting for the formation of hydrocarbons especially methane and tar [10–12] hence sensibly predicting the syngas composition. To reduce the number of sub processes and simplify the model, the following assumptions were made.

- Zero-dimensional reactor,
- Steady state process with no heat losses,
- N, Cl and S are converted to NH_3, HCl and H_2S respectively,
- Char contains only carbon and ash,
- Instantaneous devolatilization of biomass,
- Tar is $C_{10}H_8$ and other hydrocarbons formed are C_2H_2, C_2H_4, C_2H_6, C_6H_6 and C_7H_8.

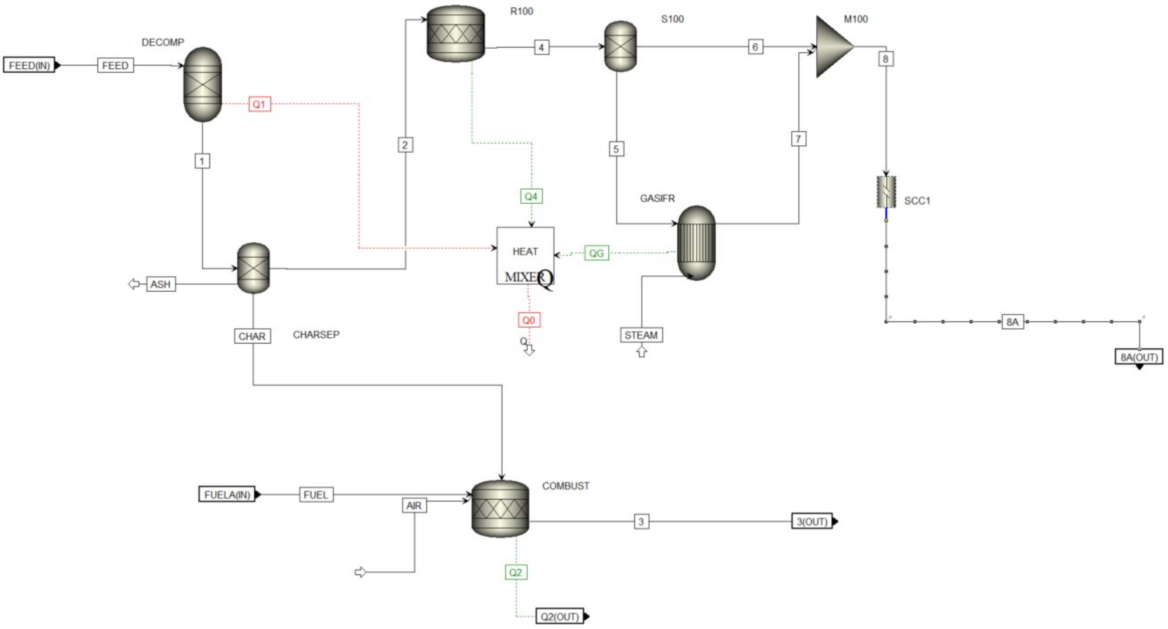

Figure B: Aspen Plus flowsheet of the dual fluidised bed gasifier model.

The Aspen Plus model of the DFB gasifier is presented in Figure B. In the DECOMP block (an RYield reactor), biomass is decomposed to its constituent elements based on the ultimate analysis of biomass. In the CHARSEP block, 15% of solid carbon is separated from the stream for combustion in the COMBUST block generate heat for the gasification reaction. In the actual gasifier, this heat is transported to the gasifier by some medium such as sand. Ash is also separated out in the CHARSEP block. The rest of the stream goes to R100, an RStoic reactor which accounts for the non-equilibrium nature of this type of gasification. In R100, a mix of tar and other hydrocarbons are formed. The hydrocarbons are separated from the stream before the GASFR block to prevent destruction in the subsequent reactor. The GASFR block is an RGibbs reactor with restricted equilibrium where steam as a gasifying agent is introduced and the gasification reactions are simulated. The stream from the GASFR is mixed with hydrocarbons stream separated earlier on in the process for a final raw syngas stream. This gasifier model is validated against experimental data from Alamia et al. [13] and presented in Table A. The model outputs are generally in good agreement with the experimental data.

Table A: Model data validated against experimental data.

	Model	**Experimental [13]**	**% Error**
H_2 (vol% dry)	42.7	42.1	1.41
CO (vol% dry)	22.6	24.1	6.64
CO_2 (vol% dry)	20.2	23.5	16.34
CH_4 (vol% dry)	8.9	8.6	3.37

C_2H_2 (vol% dry)	0.13	0.13	0
C_2H_4 (vol% dry)	2.1	2.0	476
C_2H_6 (vol% dry)	0.196	0.19	3.06
C_3H_6 (vol% dry)	-	0.001	-
Tar (g/Nm^3)	6.88	7	1.74
BTX (g/Nm^3)	3.14	3	4.46

S.2.2 Entrained gasifier model

An Aspen plus flowsheet of the entrained gasifier model used in this study is depicted in Figure C. The entrained gasifier model in this study is modelled according to the methodology presented in Field and Brasington [14] and Swanson et al. [15]. With the gasifier operating at 1300°C, the gasifier is assumed to be operating at equilibrium [15,16] and is modelled as an RGibbs reactor using the equilibrium approach. However, a temperature approach of -10°C (in quench mode) is applied to the water-gas shift reaction because there is a temperature difference between the equilibrium reaction temperature of the WGS reaction and the gasifier exit temperature [17]; also, the WGS equilibrium reaction temperature is dependent on the rate of cooling. The model has been validated against experimental data [18] (see Table B) making it suitable to be used in this study. There Is a significant difference In the methane and H_2S prediction but these represent only a small potion of the syngas and this difference Is not expected to have a significant effect on the mass balances and the economics.

Table B: Entrained gasifier model validation.

	Model	**Experiment data** [18]	**% Error**
Ar (vol%)	0.007	-	-
CH_4 (vol%)	0.0001	0.003	96.67
CO (vol%)	0.39	0.41	4.88
CO_2 (vol%)	0.105	0.102	2.94
COS (vol%)	0	-	-
H_2 (vol%)	0.295	0.298	1.01
H_2O (vol%)	0.186	0.171	8.77
H_2S (vol%)	0.007	0.011	36.36
N_2 (vol%)	0.009	0.008	12.50
NH_3 (vol%)	0	-	-
Equilibrium constant of WGS	0.426	0.427	0.234

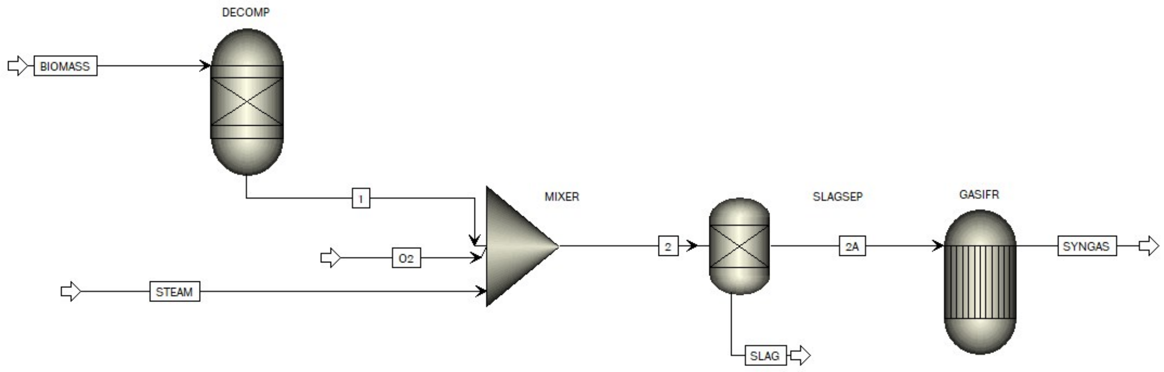

Figure C: Aspen Plus flowsheet of the entrained gasifier model.

The DECOMP block is an RYield reactor where biomass is converted from a non-conventional component to conventional elements (C, H, O, N, S, Cl) based on the ultimate analysis of the biomass feed. Biomass is mixed with the gasifying agents – steam and oxygen – based on steam to oxygen ratio and oxygen to carbon ratio for the investigated case in a mixer and sent to a SEP block to remove the ash content. Finally, the elements are sent to an RGibbs block labelled GASIFR where the gasification reactions occur using the restricted equilibrium approach.

S.3 Syngas cleaning and conditioning

The syngas cleaning and conditioning section is presented in Figure C. Wet scrubbing to remove impurities in the syngas is modelled as a flash unit using information from Field and Brasington [14]. The water flow is adjusted by a design specification to ensure the unit is in adiabatic mode and a calculator block sets the operating temperature to 5°C below the dewpoint of the incoming stream. The sour water-gas shift reactor is modelled in one stage instead of the two stages in Field and Brasington [14] due to the requirements downstream. As the syngas is intended for fuel synthesis instead of power generation, one reactor is sufficient to adjust the ratio. A splitter is added after the scrubber to split the syngas into two streams. The ratio of the split is set by a design specification to ensure that the final mixed stream has the necessary H_2/CO ratio; this also helps to control the temperature of the exothermic WGS reaction, minimise the reactor size and the amount of catalyst required. The WGS reactor inlet stream is warmed up using the outlet stream to a temperature that is 15°C above the dew point of the inlet stream. The WGS reactor is an adiabatic equilibrium reactor.

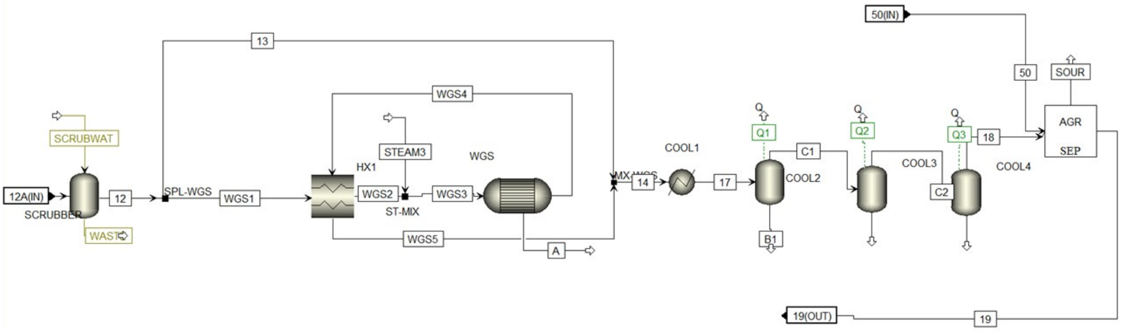

Figure D: Aspen Plus flowsheet for syngas cleaning and conditioning.

After the WGS reactor, syngas is cooled in a series of adiabatic flash units at 100°C, 60°C, and 39°C. Water condensate in the syngas is removed at each stage.

S.4 Fischer Tropsch synthesis

The FTS reactor is modelled according to the work of Swanson et al. [15]. Detailed information including the equations used in the calculator block for FTS distribution of the products can be found in [19].

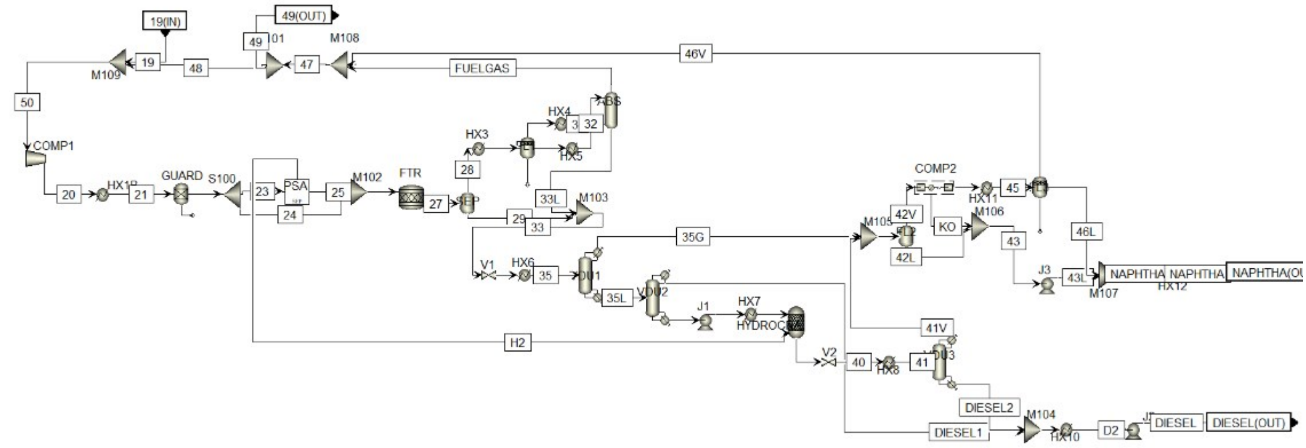

Figure E: Aspen Plus flowsheet of FTS.

The fuel from the FTS reactor needs to undergo separation. An adiabatic two-phase flash unit is first used to separate the unconverted syngas from the products. The unconverted syngas is cooled and goes into an adiabatic three-phase flash for further product separation; the resulting streams are water, unconverted syngas, and the lighter end of the FT-fuel. The lighter end of the FT-fuel and the unconverted syngas from the second flash unit are chilled and sent to an absorber to recover the rest of the FT-fuel from the unconverted syngas. The majority of the latter (~75% mass basis is recycled to the FT reactor while the balance is sent to the CHP unit. The FT-fuel from both the first flash unit and the absorber are combined in a mixer block for separation into naphtha and diesel in a series of distillation columns. The distillation columns (DC) to separate the FT-fuel into naphtha and diesel are modelled using RADRAC columns. The number of stages, reflux ratio, and bottoms rate were first estimated using the DSTWU columns. These first estimates were used in designing the RADFRAC columns, and the bottoms rates were varied to achieve >99.5% recovery of the desired products. The results of the columns are shown in Table C.

Table C: Specifications of distillation columns in FTS.

	DC1	DC2	DC3
Purpose	Separate naphtha from diesel and wax	Separate diesel from wax	Separate cracked wax into naphtha and diesel
Number of stages	30	10	20
Reflux ratio	1.32	1.72	2.65
Bottoms rate (kmol/hr)	32.54	11.35	13.28

S.5 Methanation

The methanation synthesis section has been modelled according to the work of Alamia et al. [13]. The thermodynamic equilibrium methanation model used in this study was compared to a kinetic model. The kinetic model was developed using kinetics from Xu and Froment [20] and a Fortran subroutine from Yu [21]. The reactions considered in the kinetics are:

$$CO + 3H_2 \rightarrow CH_4 + H_2O \quad (1)$$

$$CO_2 + H_2 \rightarrow CO + H_2O \quad (2)$$

$$CO_2 + 4H_2 \rightarrow CH_4 + 2H_2O \quad (3)$$

$$2CO + 5H_2 \rightarrow C_2H_6 + 2H_2O \quad (4)$$

The results after three reactors are presented in Table D. In the thermodynamic model, there is one more reactor and there is no recycling after the first reactor. Due to the similarities in both models, and to reduce convergence time, the thermodynamic equilibrium model was used in this study.

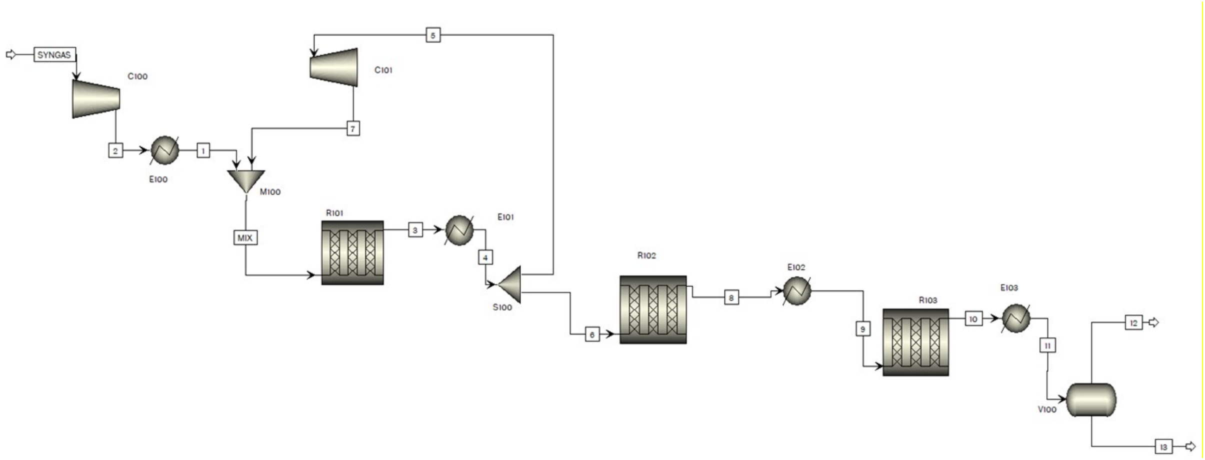

Figure F: Aspen Plus kinetic model of methanation.

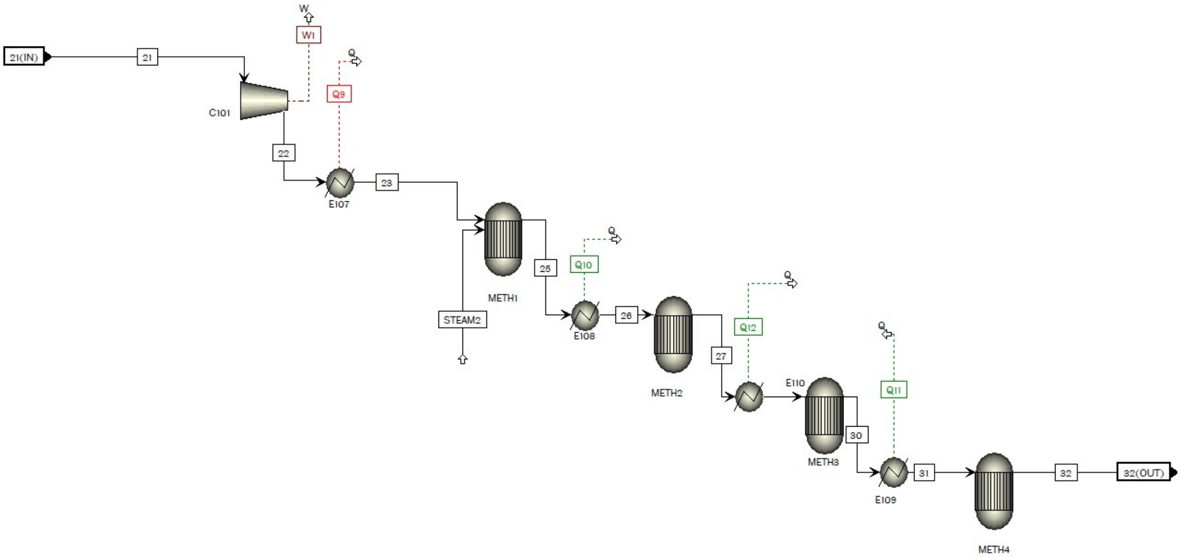

Figure G: Aspen Plus thermodynamic model of methanation.

The methanation reactors are modelled as adiabatic reactors in series with interstage cooling. In the first reactor, steam is added to prevent the formation of carbon on the catalyst [13]. The amount of steam added is determined by a design specification. The streams in between are cooled to 200°C and used to generate steam.

Table D: Comparison of the percentage conversion after each reactor between the kinetic model and the thermodynamic equilibrium model for methanation.

		Kinetic	**Thermodynamic**
Reactor 1	CO	31.3%	29.8%
	CO_2	22.5%	21%
	H_2	52.2%	51.1%

Reactor 2	CO	82.7%	81.9%
	CO_2	24.8%	21%
	H_2	84%	81.7%
Reactor 3	CO	98.1%	97.6%
	CO_2	26.5%	21.5%
	H_2	96.7%	93.5%

S.6 OMEx synthesis

S.6.1 Methanol

The details for modelling methanol synthesis according to the ICI Synetix process are available in the document 'Aspen Plus Methanol Modelling Synthesis' found in the Aspen Plus database. The operating conditions are based on the SRI Process Economics Report 43D "Mega Methanol Plants" [22]. The model is based on reaction kinetics from Vanden Bussche and Froment [23]. The Aspen document describes the process in detail; it also presents the reaction kinetics and the model validation in detail. A kinetic model based on the details from the report was completed and a thermodynamic equilibrium model was derived from it to simplify the model and reduce the convergence time. The reactions considered in the kinetic model are:

$$CO + H_2O \leftrightarrow CO_2 + H_2 \quad (5)$$

$$CO_2 + 3H_2 \leftrightarrow CH_3OH + H_2O \quad (6)$$

$$2CO + 4H_2 \rightarrow C_2H_5OH + H_2O \quad (7)$$

$$2CH_3OH \rightarrow C_2H_6O + H_2O \quad (8)$$

Table E: Comparison of the final stream composition from kinetic and thermodynamic methanol synthesis modelling

	Kinetic	**Thermodynamic**
CO (vol%)	0.007	0.005
CO_2 (vol%)	0.50	0.40
H_2 (vol%)	0.34	0.37
H_2O (vol%)	18.20	18.30
MeOH (vol%)	80.60	80.60

The temperature of the thermodynamic model was set at 250°C, which is the exit temperature of the fourth reactor. In both models, a purge stream (stream 29), which 1% of the recycle was introduced to enable computation. The results of both models are compared in Table D. The similarity in the results indicates the suitability of the thermodynamic equilibrium model for this study and similar to the bioSNG we selected the equilibrium model to reduce computational time.

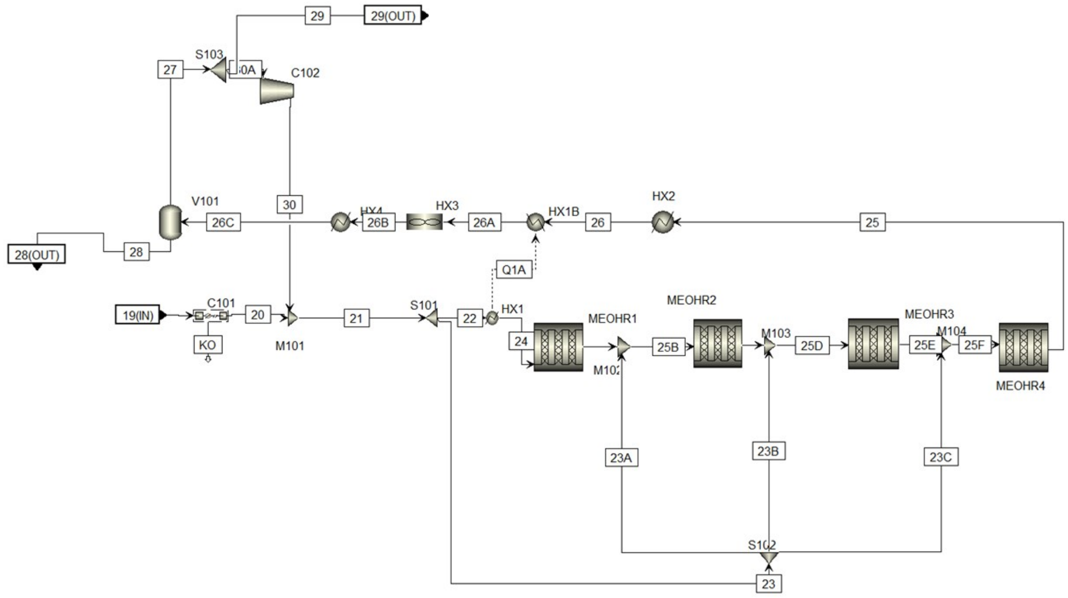

Figure H: Aspen Plus kinetic model of methanol synthesis

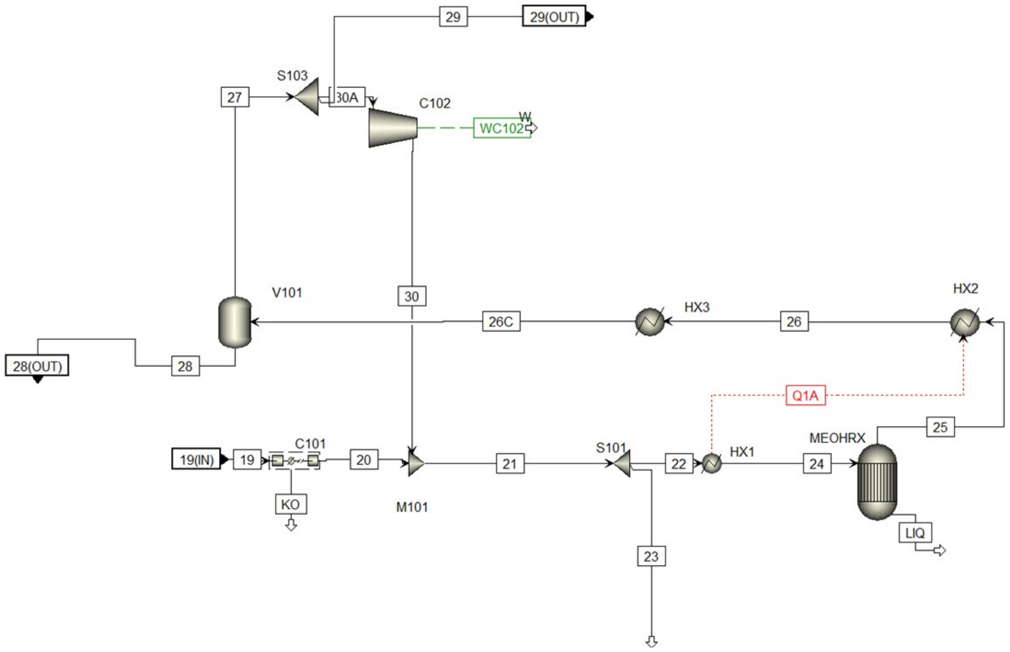

Figure I: Aspen plus thermodynamic model of methanol synthesis.

S.6.2 Formaldehyde synthesis

Formaldehyde synthesis is modelled in an adiabatic equilibrium reactor. In this reactor, methanol is dehydrated to formaldehyde. Before the reactor, a splitter removes a fraction of the methanol using a design specification to ensure that the methanol and formaldehyde going into OMEx synthesis have the same mass fraction as specified in Ai [24]. In the formaldehyde reactor, oxygen is added via air and the conversion of methanol to formaldehyde is set at 87% which is a common conversion in formaldehyde synthesis over silver catalysts [25]. Due to the exothermic nature of the reaction, heat from the exit stream is recovered to generate steam for the plant. Absorption of formaldehyde using water is simulated using a common separator block. The quantity of water used in the process is set by a design specification to ensure 37%wt FA in the resulting stream as is the requirement for the OMEx synthesis in Zhang [26] and Ai [27].

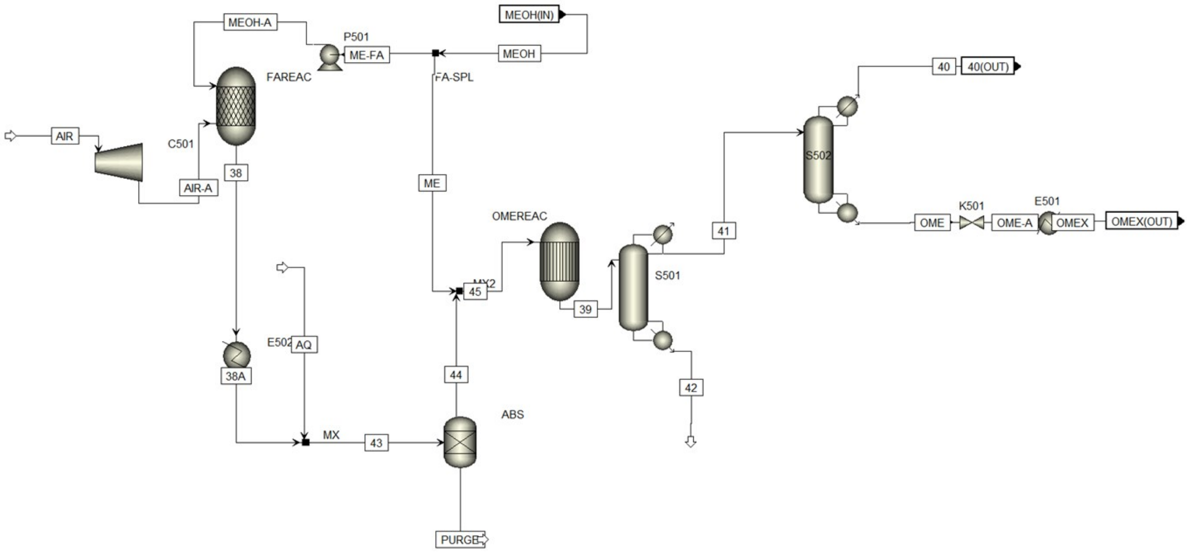

Figure J: Aspen Plus flowsheet of OMEx synthesis from methanol

S.6.3 OMEx synthesis

The OMEx synthesis was modelled based on previous experimental and modelling results available in literature. OMEx synthesis is modelled in an RYield reactor and the distribution of the products are calculated from the mass balance presented in the work of Ai [27].

Table F: Distribution of OMEx products.

Product	Mass yield
OME_3	0.433825333
OME_4	0.007346855
OME_5	0.000001003
Methanol	0.000166213
Formaldehyde	0.001142909
H_2O	0.557517687

S.7 Power generation

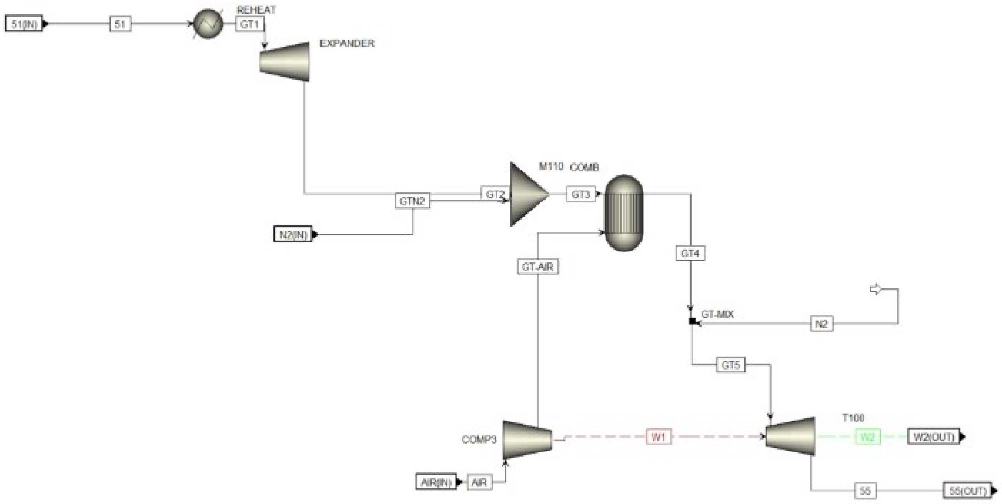

Figure K: Aspen Plus model of the gas turbine.

Power is generated in a combined cycle to provide electricity to meet some of the plants demand. In FTS and OMEx synthesis, nitrogen from the air separation is added to syngas to achieve the 4.81 MJ/Nm^3 LHV based on the NETL report [28]. The flue gas stream before the gas turbine is mixed with either compressed air or nitrogen to cool the stream to an acceptable temperature (1370°C) for the gas turbine. In methanation, there is no ASU so compressed air was used. In FTS and OMEx synthesis, the amount of nitrogen required for cooling was less than the leftover after nitrogen was used to dilute syngas, so only nitrogen was used. Where compressed air was used as the coolant, the compressed air was split into two; one part goes to the combustion chamber while the other part is used to cool down the flue gas. The amount of air required to achieve this temperature was calculated and added to the stoichiometric amount of air required for combustion and a 10% excess to ensure complete combustion. The combustion chamber is a RGibbs reactor operating adiabatically, and the discharge pressure of the gas turbine was set at 1.05 bar.

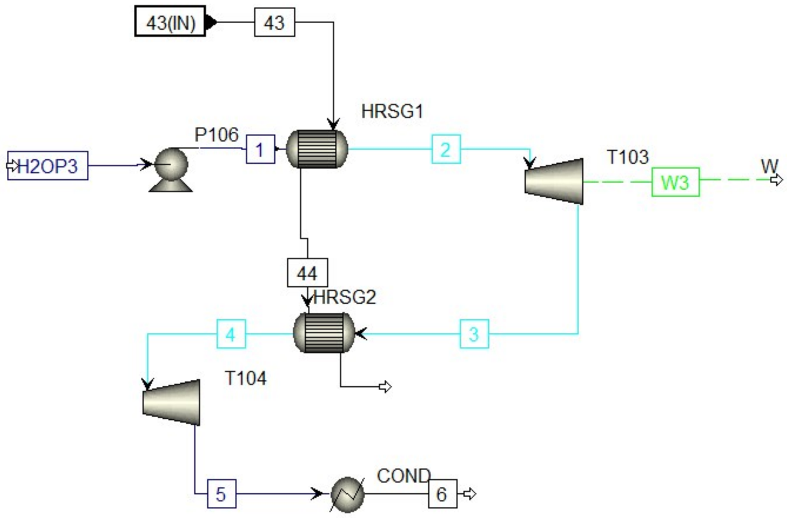

Figure L: Aspen Plus model of the steam cycle.

In the steam cycle, power was generated from a medium-pressure turbine and a low-pressure turbine. The water inlet pressure varied between 8 bar and 15 bar and heated with the flue gas in a heat exchanger with a temperature approach of 10°C. The discharge pressure of the medium-pressure turbine was set at 5 bar and exit stream was reheated with the flue gas stream before the low-pressure turbine. The discharge pressure of the low-pressure turbine was set 0.06 bar (1 psi) and the exit stream was sent to a condenser to bring the vapour fraction to 0 before recycling (not modelled) to the pump.

S.8 CO_2 compression

As depicted in Figure M, a number of stages of compression are required before optimal conditions are attained for transport of the CO_2, i.e. final pressure of 110 bar and water content of 1ppm [29]. The design of the compression section consists of three compressors with intermediate cooling followed by a pump and a final cooling stage. A typical molecular sieve configuration is also considered for water removal purposes; this step is modelled as a black box unit by employing a common separators and specifying a water content of 1ppm for the CO_2 gas stream [29]. The CO_2 stream exits the 1st compressor at 6.3 bar and 162°C, the 2nd at 22.43 bar and 149°C and the 3rd at 80 bar and 180°C while the pump raises the pressure to 110 bar.

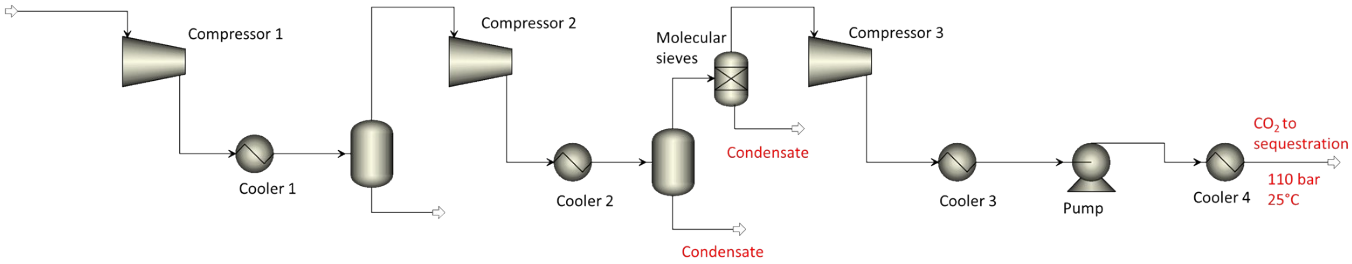

Figure M: Aspen Plus flowsheet of CO_2 compression.

S.9 Heat Integration

Heat integration on each plant was completed in order to minimise the heating and cooling utilities using the Aspen Energy Analyser, an online pinch analysis tool [30]. The minimum temperature was set at 10°C. Depending on the temperature range of the stream, heating utilities supplied were low pressure steam (2.3 bar), medium pressure steam (8.9 bar), and high pressure steam (39.8 bar) while the cooling utilities were water and air. It can be seen from Table G that after heat Integration for the BioSNG case there is no need for heating while for the FTS and the OMEx heating reductions of 58.8% and 37.8% were achieved, respectively.

Table G: Results of heat integration.

	FTS		BioSNG		OMEx	
	Before	After	Before	After	Before	After
Heating Duty (MW)	49.81	20.51	40.92	0	78.67	51.30
Cooling Duty (MW)	29.44	0.135	103.13	62.25	72.25	44.88

References

[1] C. Aichernig, H. Hofbauer, R. Rauch, R. Koch, Biomass Chp Plant Güssing : Successful Demonstration of the Steam Gasification Process, (1991) 1–4.

[2] E4Tech, Review of Technologies for Gasification of Biomass and Wastes Final report, NNFCC Bioeconomy Consult. (2009) 1–130. http://www.e4tech.com/wp-content/uploads/2016/01/gasification2009.pdf%0Ahttp://www.nnfcc.co.uk/tools/review-of-technologies-for-gasification-of-biomass-and-wastes-nnfcc-09-008.

[3] H. Thunman, M. Seemann, T. Berdugo Vilches, J. Maric, D. Pallares, H. Ström, G. Berndes, P. Knutsson, A. Larsson, C. Breitholtz, O. Santos, Advanced biofuel production via gasification – lessons learned from 200 man-years of research activity with Chalmers' research gasifier and the GoBiGas demonstration plant, Energy Sci. Eng. (2018). https://doi.org/10.1002/ese3.188.

[4] L.P.R. Pala, Q. Wang, G. Kolb, V. Hessel, Steam gasification of biomass with subsequent syngas adjustment using shift reaction for syngas production: An Aspen Plus model, Renew. Energy. 101 (2017) 484–492. https://doi.org/10.1016/j.renene.2016.08.069.

[5] N. Jand, V. Brandani, P.U. Foscolo, Thermodynamic limits and actual product yields and compositions in biomass gasification processes, Ind. Eng. Chem. Res. 45 (2006) 834–843. https://doi.org/10.1021/ie050824v.

[6] G. Gautam, S. Adhikari, S. Bhavnani, Estimation of biomass synthesis gas composition using equilibrium modeling, in: Energy and Fuels, 2010. https://doi.org/10.1021/ef901477c.

[7] P. Kaushal, J. Abedi, N. Mahinpey, A comprehensive mathematical model for biomass gasification in a bubbling fluidized bed reactor, Fuel. 89 (2010) 3650–3661. https://doi.org/10.1016/j.fuel.2010.07.036.

[8] Y. Wang, C.M. Kinoshita, Kinetic model of biomass gasification, Sol. Energy. 51 (1993) 19–25. https://doi.org/10.1016/0038-092X(93)90037-O.

[9] R. Radmanesh, J. Cnaouki, C. Guy, Biomass gasification in a bubbling fluidized bed reactor: Experiments and modeling, AIChE J. (2006). https://doi.org/10.1002/aic.11020.

[10] K.D. Panopoulos, L.E. Fryda, J. Karl, S. Poulou, E. Kakaras, High temperature solid oxide fuel cell integrated with novel allothermal biomass gasification. Part I: Modelling and feasibility study, J. Power Sources. 159 (2006) 570–585. https://doi.org/10.1016/j.jpowsour.2005.12.024.

[11] G. Schuster, G. Löffler, K. Weigl, H. Hofbauer, Biomass steam gasification - An extensive parametric modeling study, Bioresour. Technol. 77 (2001) 71–79. https://doi.org/10.1016/S0960-8524(00)00115-2.

[12] W. Doherty, A. Reynolds, D. Kennedy, Aspen plus simulation of biomass gasification in a steam blown dual fluidised bed, Mater. Process Energy. (2013) 212–220.

[13] A. Alamia, S. Òsk Gardarsdòttir, A. Larsson, F. Normann, H. Thunman, Efficiency Comparison of Large-Scale Standalone, Centralized, and Distributed Thermochemical Biorefineries, Energy Technol. 5 (2017) 1435–1448. https://doi.org/10.1002/ente.201600719.

[14] R.P. Field, R. Brasington, Baseline flowsheet model for IGCC with carbon capture, Ind. Eng. Chem. Res. (2011). https://doi.org/10.1021/ie200288u.

[15] R.M. Swanson, A. Platon, J.A. Satrio, R.C. Brown, Techno-economic analysis of biomass-to-liquids production based on gasification, Fuel. 89 (2010) S11–S19. https://doi.org/10.1016/j.fuel.2010.07.027.

[16] H.C. Frey, N. Akunuri, Probabilistic Modeling and Evaluation of the Performance, Emissions, and Cost of Texaco Gasifier-Based Integrated Gasification Combined Cycle Systems Using ASPEN, 2001.

[17] M. Bockelie, M. Denison, Z. Chen, C. Senior, A. Sarofim, Using Models To Select Operating Conditions for Gasifiers, (2003).

[18] A.P. Watkinson, J.P. Lucas, C.J. Lim, A prediction of performance of commercial coal gasifiers, Fuel. 70 (1991) 519–527. https://doi.org/10.1016/0016-2361(91)90030-E.

[19] R.M. Swanson, A. Platon, J.A. Satrio, R.C. Brown, Techno-economic analysis of biomass-to-liquids production based on gasification scenarios, ACS Natl. Meet. B. Abstr. (2009).

[20] J. Xu, G.F. Froment, Methane steam reforming, methanation and water-gas shift: I. Intrinsic

kinetics, AIChE J. 35 (1989) 88–96. https://doi.org/10.1002/aic.690350109.

[21] B.Y. Yu, I.L. Chien, Design and economic evaluation of a coal-to-synthetic natural gas process, Ind. Eng. Chem. Res. 54 (2015) 2339–2352. https://doi.org/10.1021/ie503595r.

[22] A. Pavone, Mega Methanol Plants, Report No. 43D, Menlo Park, California, 2003.

[23] K.M. Vanden Bussche, G.F. Froment, A Steady-State Kinetic Model for Methanol Synthesis and the Water Gas Shift Reaction on a Commercial Cu/ZnO/Al 2 O 3 Catalyst, 1996.

[24] Z.J. Ai, C.Y. Chung, I.L. Chien, Design and Control of Poly(Oxymethylene) Dimethyl Ethers Production Process Directly From Formaldehyde and Methanol in Aqueous Solutions, IFAC-PapersOnLine. 51 (2018) 578–583. https://doi.org/10.1016/j.ifacol.2018.09.362.

[25] G.J. Millar, M. Collins, Industrial Production of Formaldehyde Using Polycrystalline Silver Catalyst, Ind. Eng. Chem. Res. 56 (2017) 9247–9265. https://doi.org/10.1021/acs.iecr.7b02388.

[26] X. Zhang, A.O. Oyedun, A. Kumar, D. Oestreich, U. Arnold, J. Sauer, An optimized process design for oxymethylene ether production from woody-biomass-derived syngas, Biomass and Bioenergy. 90 (2016) 7–14. https://doi.org/10.1016/j.biombioe.2016.03.032.

[27] Z.J. Ai, C.Y. Chung, I.L. Chien, Design and Control of Poly(Oxymethylene) Dimethyl Ethers Production Process Directly From Formaldehyde and Methanol in Aqueous Solutions, IFAC-PapersOnLine. 51 (2018) 578–583. https://doi.org/10.1016/j.ifacol.2018.09.362.

[28] T. Fout, A. Zoelle, D. Keairns, M. Turner, M. Woods, N. Kuehn, V. Shah, V. Chou, L. Pinkerton, Cost and Performance Baseline for Fossil Energy Plants Volume 1a: Bituminous Coal (PC) and Natural Gas to Electricity Revision 3, 2015. https://doi.org/DOE/NETL-2010/1397.

[29] Politecnico di Milano - Alstom UK, CArbon-free Electricity by SEWGS: Advanced materials, Reactor-, and process design, D 4.9 European best practice guidelines for assessment of CO2 capture technologies, 2008.

[30] J.S. Umbach, Online Pinch Analysis Tool, (2010). http://www.uic-che.org/pinch/index.php (accessed March 22, 2021).